

Jeffrey A. Fessler

EECS Dept., BME Dept., Dept. of Radiology  
University of Michigan

`web.eecs.umich.edu/~fessler`

Fully 3D Conference

02 June 2015

(and a bit of PET and SPECT)

Jeffrey A. Fessler

EECS Dept., BME Dept., Dept. of Radiology  
University of Michigan

`web.eecs.umich.edu/~fessler`

Fully 3D Conference

02 June 2015

- Research support from GE Healthcare
- Supported in part by NIH grants P01 CA-87634, U01 EB018753
- Equipment support from Intel Corporation

## **Acknowledgment:**

many collaborators and many students and post-docs

## What

CT

MRI

## Why

Why CT iterative

Why MRI iterative

## How

Optimization transfer

Separable quadratic surrogates

Momentum

Ordered subsets

## Parallelization

## What

CT

MRI

## Why

Why CT iterative

Why MRI iterative

## How

Optimization transfer

Separable quadratic surrogates

Momentum

Ordered subsets

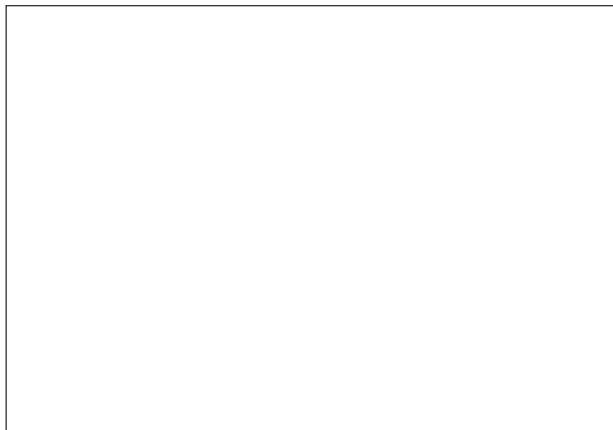
## Parallelization



CT image reconstruction problem:

Determine unknown attenuation map  $\mathbf{x}$  given sinogram data  $\mathbf{y}$  using system matrix  $\mathbf{A}$ .

*cf.* SPECT with orbiting gamma camera

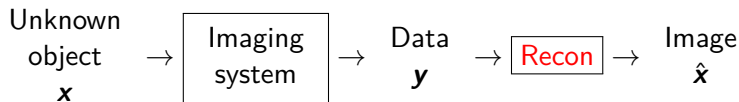


(No moving parts  
to animate)

MR image reconstruction problem:

Determine unknown magnetization image  $\mathbf{x}$  given k-space data  $\mathbf{y}$   
using system matrix  $\mathbf{A}$

Defer motion for now...



How to reconstruct object  $\mathbf{x}$  from data  $\mathbf{y}$ ?

## Non-iterative methods:

- analytical / direct
  - Filtered back-projection (FBP) for CT (textbook: Radon transform)
  - Inverse FFT for MRI (textbook: FFT)
- idealized description of the system (“textbook model”)
  - geometry / sampling
  - disregards noise and simplifies physics
- typically fast

## Iterative methods:

- model-based / statistical
- based on “reasonably accurate” models for physics and statistics
- usually much slower

- A picture is worth 1000 words
- (and perhaps several 1000 seconds of computation?)



Thin-slice FBP  
Seconds

ASIR (denoise)  
A bit longer

Statistical  
Much longer

(Same sinogram, so all at same **dose**)

## What

CT

MRI

## Why

Why CT iterative

Why MRI iterative

## How

Optimization transfer

Separable quadratic surrogates

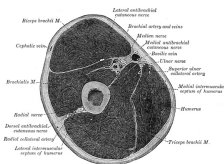
Momentum

Ordered subsets

## Parallelization

- Accurate **physics** models
  - X-ray spectrum, beam-hardening, scatter, ...  
⇒ reduced artifacts? quantitative CT?
  - X-ray detector spatial response, focal spot size, ...  
⇒ improved spatial resolution?
  - detector spectral response (e.g., photon-counting detectors)  
⇒ improved contrast between distinct material types?
- Nonstandard **geometries**
  - transaxial truncation (wide patients)
  - long-object problem in helical CT
  - irregular sampling in “next-generation” geometries
  - coarse angular sampling in image-guidance applications
  - limited angular range (tomosynthesis)
  - “missing” data, e.g., bad pixels in flat-panel systems

- Appropriate models of (data dependent) measurement **statistics**
  - weighting reduces influence of photon-starved rays (*cf.* FBP)  
⇒ reducing image noise or X-ray **dose**
- **Object** constraints / priors
  - nonnegativity
  - object support
  - piecewise smoothness
  - object sparsity (e.g., angiography)
  - sparsity in some basis
  - motion models
  - dynamic models
  - ...



Henry Gray, *Anatomy of the Human Body*, 1918, Fig. 413.

Constraints may help reduce image artifacts or noise or **dose**.

Similar motivations/benefits in PET and SPECT.

- ▶ Computation **time**
- ▶ Must reconstruct entire FOV
- ▶ Complexity of models and software
- ▶ Algorithm **nonlinearities**
  - Difficult to analyze resolution/noise properties (*cf.* FBP)
  - Tuning parameters
  - Challenging to characterize performance / assess IQ

3D helical X-ray CT scan of abdomen/pelvis:

100 kVp, 25-38 mA, 0.4 second rotation, 0.625 mm slice, 0.6 mSv.



FBP



ASIR



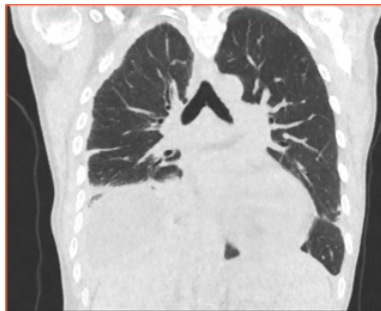
Statistical

Helical chest CT study with dose = 0.09 mSv.  
Typical CXR effective dose is about 0.06 mSv.

(Health Physics Soc.: <http://www.hps.org/publicinformation/ate/q2372.html>)



FBP



MBIR

Veo (MBIR) images courtesy of Jiang Hsieh, GE Healthcare

# History: Statistical reconstruction for X-ray CT\*

- Iterative method for X-ray CT (Hounsfield, 1968)
- ART for tomography (Gordon, Bender, Herman, JTB, 1970)
- ...
- Roughness regularized LS for tomography (Kashyap & Mittal, 1975)
- Poisson likelihood (transmission) (Rockmore and Macovski, TNS, 1977)
- EM algorithm for Poisson transmission (Lange and Carson, JCAT, 1984)
- Iterative coordinate descent (ICD) (Sauer and Bouman, T-SP, 1993)
- Ordered-subsets algorithms (Manglos *et al.*, PMB 1995)  
(Kamphuis & Beekman, T-MI, 1998)  
(Erdoğan & Fessler, PMB, 1999)
- ...
- Commercial OS for Philips BrightView SPECT-CT (2010)
- Commercial ICD for GE CT scanners (circa 2010)
- FDA 510(k) clearance of Veo (Sep. 2011)
- First Veo installation in USA (at UM) (Jan. 2012)

(\* numerous omissions, including many denoising methods)

Optimization problem formulation:  $\hat{\mathbf{x}} = \arg \min_{\mathbf{x} \geq 0} \Psi(\mathbf{x})$

$$\underbrace{\Psi(\mathbf{x})}_{\text{cost function}} \triangleq \underbrace{\frac{1}{2} \|\mathbf{y} - \mathbf{A}\mathbf{x}\|_{\mathbf{W}}^2}_{\text{data-fit term physics \& statistics}} + \underbrace{\beta \sum_{j=1}^N \sum_{k \in \mathcal{N}_j} \psi(x_j - x_k)}_{\text{regularizer prior models}}$$

$\mathbf{y}$  : measured data (sinogram)

$\mathbf{A}$  : system matrix (physics / geometry)

$\mathbf{W}$  : weighting matrix (statistics)

$\mathbf{x}$  : unknown image (attenuation map)

$\beta$  : regularization parameter(s)

$\mathcal{N}_j$  : neighborhood of  $j$ th voxel

$\psi$  : edge-preserving potential function

(piece-wise smoothness / gradient sparsity)

$$\hat{\mathbf{x}} = \arg \min_{\mathbf{x} \geq \mathbf{0}} \Psi(\mathbf{x}), \quad \Psi(\mathbf{x}) \triangleq \frac{1}{2} \|\mathbf{y} - \mathbf{Ax}\|_{\mathbf{W}}^2 + \sum_j \sum_k \beta_{j,k} \psi(x_j - x_k)$$

## Apparent topics:

- regularization design / parameter selection  $\psi, \beta_{jk}$
- statistical modeling  $\mathbf{W}, \|\cdot\|$
- system modeling  $\mathbf{A}$
- optimization algorithms (arg min)
- assessing IQ of  $\hat{\mathbf{x}}$

## Other topics:

- system design
- motion
- spectral
- dose ...

Inverse FFT is fast (like FBP). Why change?

(Joint work with D. Noll, J. Nielsen, ...)

Recall rationale for CT/PET/SPECT:

- ▶ **physics** modeling
  - reduce artifacts
  - improve resolution
  - improve contrast
- ▶ **noise** modeling: (dose, variability)
- ▶ **sampling**: non-standard geometries
- ▶ **constraints** on object

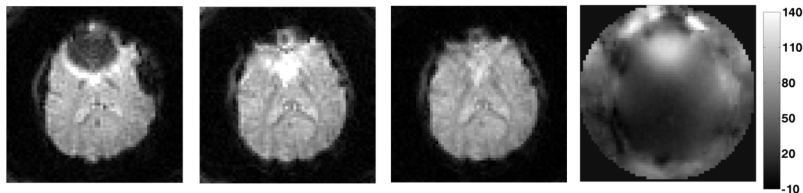
Which of these matter for MRI?

# MRI why iterative: Physics

Physics modeling (e.g., field inhomogeneity)  $\implies$  reduced artifacts

Example: T2\*-weighted imaging

(Sutton *et al.*, IEEE T-MI, 03)



uncorrected

traditional

iterative

field map

$$\hat{\mathbf{x}} = \arg \min_{\mathbf{x}} \frac{1}{2} \|\mathbf{y} - \mathbf{Ax}\|_2^2 + \beta R(\mathbf{x})$$

System matrix  $\mathbf{A}$  depends on (measured) field map:

$$a_{ij} = e^{-i\omega_j t_i} e^{-i2\pi \vec{v}_i \cdot \vec{r}_j}$$

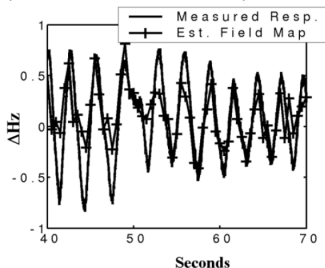
No analytical inverse of  $\mathbf{A}$ . *cf.* nonuniform attenuation correction in SPECT

Joint estimation of field map  $\omega$  and magnetization image  $\mathbf{x}$ :

$$(\hat{\mathbf{x}}, \hat{\omega}) = \arg \min_{\mathbf{x}, \omega} \frac{1}{2} \|\mathbf{y} - \mathbf{A}(\omega)\mathbf{x}\|_2^2 + \beta_1 R_1(\mathbf{x}) + \beta_2 R_2(\omega)$$

Useful when field map drifts in dynamic imaging.

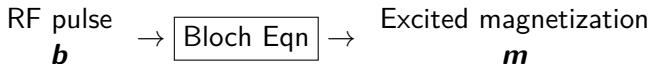
(Sutton *et al.*, MRM 04) (Olafsson *et al.*, T-MI 08)



*cf.* joint estimation of attenuation map  $\mu$  and activity image  $\lambda$  in SPECT, PET and TOF-PET.

(Censor *et al.*, T-NS 79) (Clinthorne *et al.*, NSS 91) (Rezaei, Defrise, Nuyts, T-MI 14)

## RF pulse design



Small-tip approximation:  $\mathbf{m} \approx \mathbf{A}\mathbf{b}$

Iterative RF pulse design (with RF power regularization):

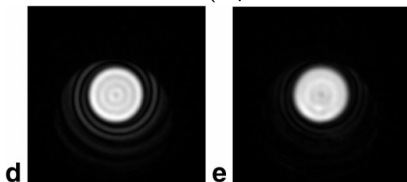
$$\arg \min_{\mathbf{b}} \|\mathbf{m} - \mathbf{A}\mathbf{b}\|_2^2 + \beta \|\mathbf{b}\|_2^2$$

Minimize using CG.

(Yip *et al.*, MRM, Oct. 2005)

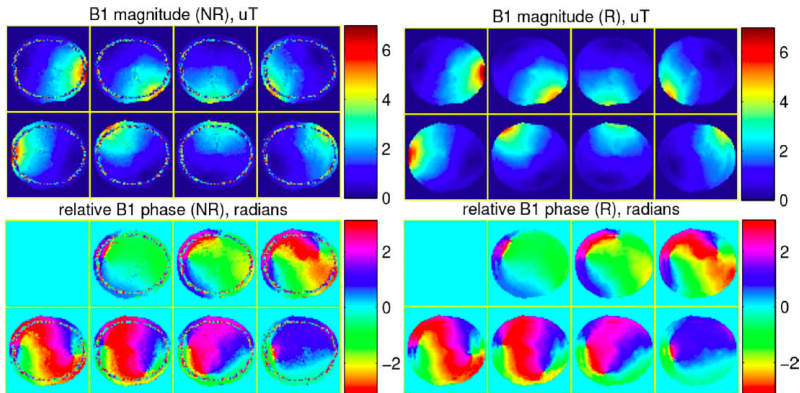
d. Non-iterative:

e. Iterative:



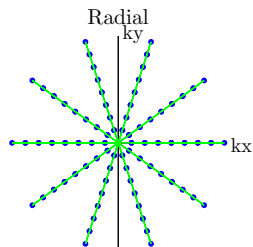
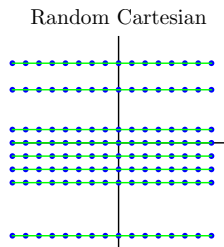
- ▶ MRI measurements: (complex) AWGN  $\implies$  easy !?

- ▶ MRI measurements: (complex) AWGN  $\implies$  easy !?
- ▶ Variance of image *phase* depends on image magnitude.
- ▶ Image phase useful in some applications, e.g., B1 mapping:



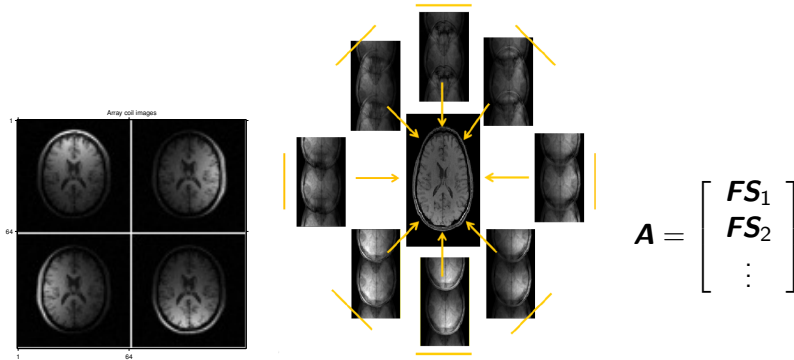
Unregularized vs regularized phase estimate. (Zhao *et al.*, T-MI 14)

- ▶ Reducing k-space sampling  $\implies$  reduced scan time
- ▶ Especially compelling for dynamic imaging (cf. CT and SPECT)
- ▶ Popular “under-sampled” patterns: (cf. sparse-view CT)



- ▶ Solution strategies
  - Multiple receive coils
  - Object model assumptions (e.g., sparsity)
  - iterative reconstruction (“compressed sensing”)

Under-sampled Cartesian k-space: use multiple receive coils with individual spatial sensitivity patterns. (Pruessmann *et al.*, MRM, 1999)



Compressed sensing parallel MRI  $\equiv$  (random) under-sampling

Lustig *et al.*, IEEE Sig. Proc. Mag., Mar. 2008

*cf.* multiple-source CT (speed) or multi-camera SPECT (counts)

Regularized estimator:

$$\hat{\mathbf{x}} = \arg \min_{\mathbf{x}} \underbrace{\frac{1}{2} \|\mathbf{y} - \mathbf{F}\mathbf{S}\mathbf{x}\|_2^2}_{\text{data fit}} + \beta \underbrace{\|\mathbf{R}\mathbf{x}\|_p}_{\text{sparsity}}.$$

$\mathbf{F}$  is under-sampled DFT matrix (wide)

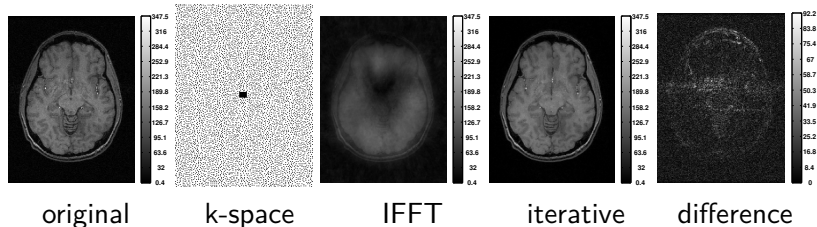
Features:

- coil sensitivity matrix  $\mathbf{S}$  is block diagonal
- $\mathbf{F}'\mathbf{F}$  is circulant (for Cartesian sampling)

Challenges:

- Data-fit Hessian  $\mathbf{S}'\mathbf{F}'\mathbf{F}\mathbf{S}$  is highly shift variant due to coil sensitivity maps
- Non-quadratic (edge-preserving) regularization  $\|\cdot\|_p$
- Non-smooth regularization  $\|\cdot\|_1$  (cf. sparse view CT)
- Complex quantities
- Large problem size (if 3D or dynamic or many coils)

Example of “compressed sensing” MRI reconstruction:



- Fully sampled body coil image of human brain ( $144 \times 128$ )
- Poisson-disk-based k-space sampling, 16% sampling (acceleration 6.25)
- Square-root of sum-of-squares inverse FFT of zero-filled k-space data for 8 coils
- Regularized reconstruction  $x^{(\infty)}$   
combined TV and  $\ell_1$  norm of two-level undecimated Haar wavelets
- Difference image magnitude

(Sathish Ramani & JF, IEEE T-MI, Mar. 2011)

# Summary of “What” and “Why”

- ▶ CT and MRI both involve inverse problems
- ▶ Some similarities in motivations and formulations
- ▶ Some similarities in computation challenges
- ▶ Some opportunities for cross-fertilization
- ▶ Caution: MRI reconstruction field is crowded!

## What

CT

MRI

## Why

Why CT iterative

Why MRI iterative

## How

Optimization transfer

Separable quadratic surrogates

Momentum

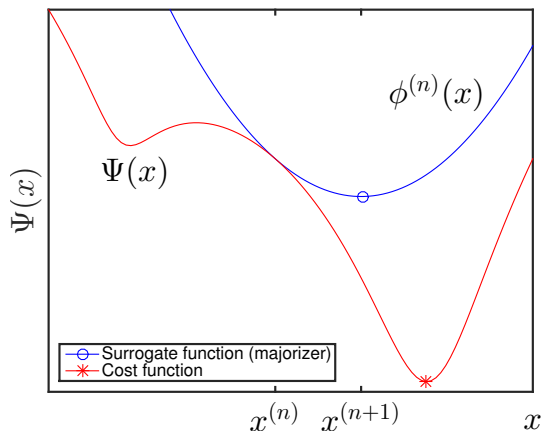
Ordered subsets

## Parallelization

$$\hat{\mathbf{x}} = \underset{\mathbf{x} \geq \mathbf{0}}{\text{arg min}} \Psi(\mathbf{x}), \quad \Psi(\mathbf{x}) \triangleq \frac{1}{2} \|\mathbf{y} - \mathbf{A}\mathbf{x}\|_{\mathbf{W}}^2 + \sum_{j=1}^N \sum_k \beta_{j,k} \psi(x_j - x_k)$$

### Optimization challenges:

- large problem size:  $\mathbf{x} \in \mathbb{R}^{512 \times 512 \times 600}$ ,  $\mathbf{y} \in \mathbb{R}^{888 \times 64 \times 7000}$
- $\mathbf{A}$  is sparse but still too large to store; compute  $\mathbf{A}\mathbf{x}$  on-the-fly
- $\mathbf{W}$  has enormous dynamic range (1 to  $\exp(-9) \approx 1.2 \cdot 10^{-4}$ )
- Gram matrix  $\mathbf{A}'\mathbf{W}\mathbf{A}$  highly shift variant
- $\Psi$  is non-quadratic but convex (and often smooth)
- nonnegativity constraint
- data size grows: dual-source CT, spectral CT, wide-cone CT, ...
- Moore's law insufficient

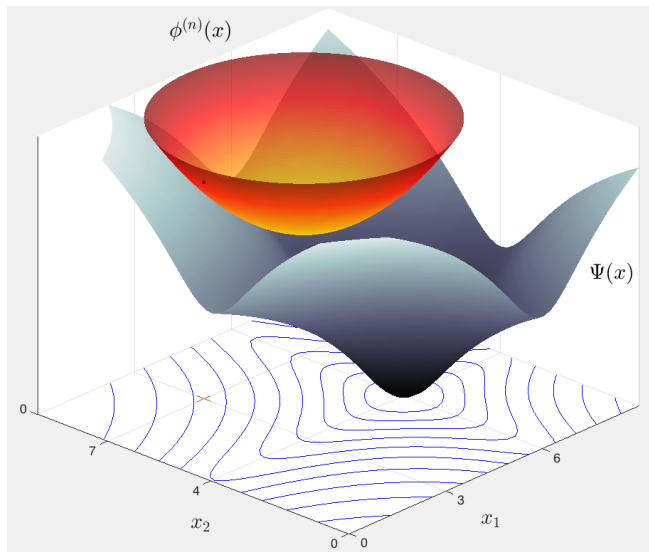


$$\phi^{(n)}(\mathbf{x}^{(n)}) = \Psi(\mathbf{x}^{(n)})$$

$$\phi^{(n)}(\mathbf{x}) \geq \Psi(\mathbf{x})$$

cf. ML-EM

$$\mathbf{x}^{(n+1)} = \arg \min_{\mathbf{x}} \phi^{(n)}(\mathbf{x})$$



## What

CT

MRI

## Why

Why CT iterative

Why MRI iterative

## How

Optimization transfer

Separable quadratic surrogates

Momentum

Ordered subsets

## Parallelization

$$\begin{aligned}
 L(\mathbf{x}) &= \frac{1}{2} \|\mathbf{y} - \mathbf{A}\mathbf{x}\|_{\mathbf{W}}^2 \\
 &= L(\mathbf{x}^{(n)}) + \nabla L(\mathbf{x}^{(n)}) (\mathbf{x} - \mathbf{x}^{(n)}) + \frac{1}{2} \underbrace{(\mathbf{x} - \mathbf{x}^{(n)})' \mathbf{A}' \mathbf{W} \mathbf{A} (\mathbf{x} - \mathbf{x}^{(n)})}_{\text{non-separable}} \\
 &\leq L(\mathbf{x}^{(n)}) + \nabla L(\mathbf{x}^{(n)}) (\mathbf{x} - \mathbf{x}^{(n)}) + \frac{1}{2} \underbrace{(\mathbf{x} - \mathbf{x}^{(n)})' \mathbf{D} (\mathbf{x} - \mathbf{x}^{(n)})}_{\text{separable}} \\
 &\triangleq \phi_{\mathbf{L}}^{(n)}(\mathbf{x}), \quad \text{a "SQS",}
 \end{aligned}$$

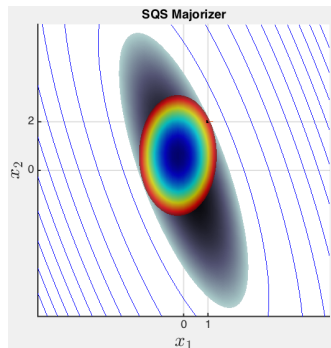
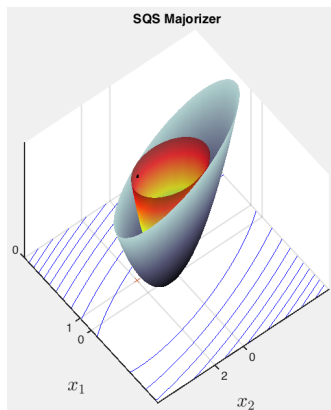
where  $\mathbf{A}' \mathbf{W} \mathbf{A} \preceq \mathbf{D} = \text{diag}\{\mathbf{A}' \mathbf{W} \mathbf{A} \mathbf{1}\}$ .

(De Pierro, T-MI, Mar. 1995)

Proofs:

- Convexity of  $x^2$
- Geršgorin disk theorem
- Cauchy-Schwarz inequality

# Separable Quadratic Surrogates (SQS): Pictures



- Find minimizer of  $L(\mathbf{x})$ : challenging
- Find minimizer of  $\phi_L^{(n)}(\mathbf{x})$ : easy (separate 1D problems)

General optimization transfer (majorize-minimize) method:

$$\mathbf{x}^{(n+1)} = \arg \min_{\mathbf{x}} \phi_{\mathbf{L}}^{(n)}(\mathbf{x})$$

For SQS:

$$\phi_{\mathbf{L}}^{(n)}(\mathbf{x}) = L(\mathbf{x}^{(n)}) + \nabla L(\mathbf{x}^{(n)})'(\mathbf{x} - \mathbf{x}^{(n)}) + \frac{1}{2} (\mathbf{x} - \mathbf{x}^{(n)})' \mathbf{D} (\mathbf{x} - \mathbf{x}^{(n)})$$

$$\nabla \phi_{\mathbf{L}}^{(n)}(\mathbf{x}) = \nabla L(\mathbf{x}^{(n)}) + \mathbf{D} (\mathbf{x} - \mathbf{x}^{(n)})$$

$$\mathbf{0} = \nabla \phi_{\mathbf{L}}^{(n)}(\mathbf{x}^{(n+1)}) = \nabla L(\mathbf{x}^{(n)}) + \mathbf{D} (\mathbf{x}^{(n+1)} - \mathbf{x}^{(n)})$$

$$\mathbf{x}^{(n+1)} = \mathbf{x}^{(n)} - \mathbf{D}^{-1} \nabla L(\mathbf{x}^{(n)})$$

“diagonally preconditioned gradient descent”

(Erdođan & JF, PMB, 1999)

Ordinary gradient descent (GD) for WLS:

$$\mathbf{x}^{(n+1)} = \mathbf{x}^{(n)} - \alpha \nabla L(\mathbf{x}^{(n)}) = \mathbf{x}^{(n)} - \alpha \mathbf{A}' \mathbf{W} (\mathbf{A} \mathbf{x}^{(n)} - \mathbf{y}),$$

where textbook step size is reciprocal of Lipschitz constant:

$$\alpha = \frac{1}{\lambda_{\max}(\mathbf{A}' \mathbf{W} \mathbf{A})}.$$

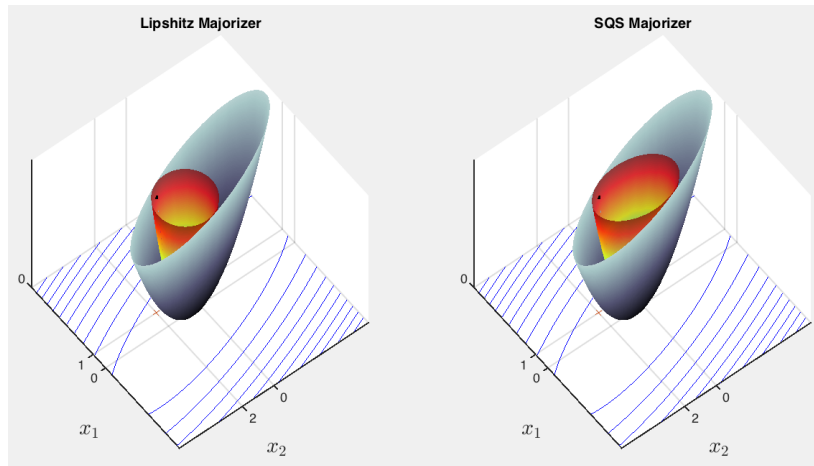
WLS-GD is equivalent to WLS-SQS with “isotropic” majorizer Hessian:

$$\mathbf{D} = \lambda_{\max}(\mathbf{A}' \mathbf{W} \mathbf{A}) \mathbf{I}.$$

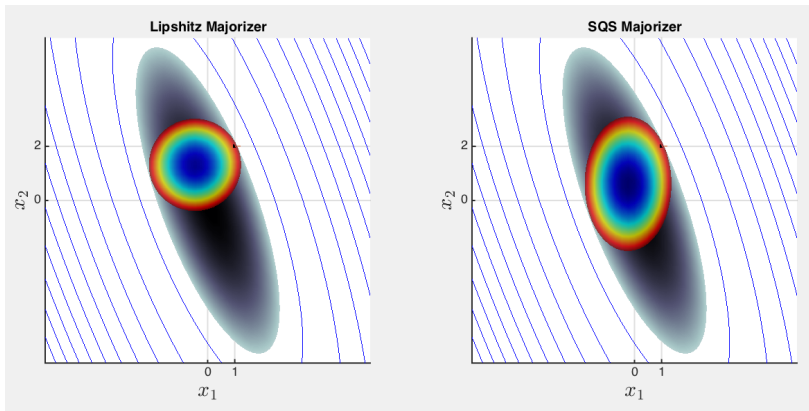
Drawbacks:

- $\lambda_{\max}(\mathbf{A}' \mathbf{W} \mathbf{A})$  usually impractical to compute (in CT)
- Usually slower convergence due to smaller step sizes

# SQS versus GD: Pictures



# SQS versus GD: Pictures



## What

CT

MRI

## Why

Why CT iterative

Why MRI iterative

## How

Optimization transfer

Separable quadratic surrogates

**Momentum**

Ordered subsets

## Parallelization

Assumptions:

- $\Psi$  is convex (need not be strictly convex)
- $\Psi$  has non-empty set of global minimizers  
 $\hat{\mathbf{x}} \in \mathcal{X}^* = \{ \mathbf{x}^{(*)} \in \mathbb{R}^N : \Psi(\mathbf{x}^{(*)}) \leq \Psi(\mathbf{x}), \forall \mathbf{x} \in \mathbb{R}^N \}$
- $\Psi$  is smooth (differentiable with  $L$ -Lipschitz gradient)  
 $\| \nabla \Psi(\mathbf{x}) - \nabla \Psi(\mathbf{z}) \|_2 \leq L \| \mathbf{x} - \mathbf{z} \|_2, \quad \forall \mathbf{x}, \mathbf{z} \in \mathbb{R}^N$

GD with step size  $1/L$  ensures monotonic descent of  $\Psi$ :

$$\mathbf{x}^{(n+1)} = \mathbf{x}^{(n)} - \frac{1}{L} \nabla \Psi(\mathbf{x}^{(n)}).$$

Drori & Teboulle (2014) derive tightest “inaccuracy” bound:

$$\underbrace{\Psi(\mathbf{x}^{(n)}) - \Psi(\mathbf{x}^{(*)})}_{\text{inaccuracy}} \leq \frac{L \| \mathbf{x}^{(0)} - \mathbf{x}^{(*)} \|_2^2}{4n + 2}.$$

For a Huber-like function  $\Psi$ , GD achieves that (tight) bound.

$O(1/n)$  rate is undesirably slow.

# Nesterov's fast gradient method (FGM1)



Nesterov (1983) iteration: Initialize:  $t_0 = 1$ ,  $\mathbf{z}^{(0)} = \mathbf{x}^{(0)}$

$$\mathbf{z}^{(n+1)} = \mathbf{x}^{(n)} - \frac{1}{L} \nabla \Psi(\mathbf{x}^{(n)}) \quad (\text{usual GD update})$$

$$t_{n+1} = \frac{1}{2} \left( 1 + \sqrt{1 + 4t_n^2} \right) \quad (\text{magic momentum factors})$$

$$\mathbf{x}^{(n+1)} = \mathbf{z}^{(n+1)} + \frac{t_n - 1}{t_{n+1}} \left( \mathbf{z}^{(n+1)} - \mathbf{z}^{(n)} \right) \quad (\text{update with momentum})$$

- ▶ Reverts to GD if  $t_n = 1, \forall n$ .
- ▶ Comparable computation as GD
- ▶ Store one additional image-sized vector  $\mathbf{z}^{(n)}$

FGM1 shown by Nesterov to be  $O(1/n^2)$  for “primary” sequence:

$$\Psi(\mathbf{z}^{(n)}) - \Psi(\mathbf{x}^{(\star)}) \leq \frac{2L \|\mathbf{x}^{(0)} - \mathbf{x}^{(\star)}\|_2^2}{(n+1)^2}.$$

Nesterov constructed a function  $\Psi$  such that any first-order method achieves

$$\frac{\frac{3}{32}L \|\mathbf{x}^{(0)} - \mathbf{x}^{(\star)}\|_2^2}{(n+1)^2} \leq \Psi(\mathbf{x}^{(n)}) - \Psi(\mathbf{x}^{(\star)}).$$

Thus  $O(1/n^2)$  rate of FGM1 is optimal.

Donghwan Kim (2014) analyzed “secondary” sequence:

$$\Psi(\mathbf{x}^{(n)}) - \Psi(\mathbf{x}^{(\star)}) \leq \frac{2L \|\mathbf{x}^{(0)} - \mathbf{x}^{(\star)}\|_2^2}{(n+2)^2}.$$

- ▶ “Traditional” iterative soft thresholding algorithm (ISTA) uses (global) Lipschitz constant of data-fit term:

$$\nabla^2 \frac{1}{2} \|\mathbf{y} - \mathbf{F}\mathbf{S}\|_2^2 = \mathbf{S}'\mathbf{F}'\mathbf{F}\mathbf{S} \leq \mathbf{S}'\mathbf{S} \leq \lambda_{\max} \mathbf{I}, \quad \lambda_{\max} = \max_j [\mathbf{S}'\mathbf{S}]_{j,j}$$

$\lambda_{\max}$  is maximum sum-of-squares value of sensitivity maps.

- ▶ Augmented Lagrangian (AL) methods converge faster than ISTA, FISTA, MFISTA (Ramani & JF, T-MI, 2011)
- ▶ **BARISTA** (B1-based, adaptive restart, ISTA) (Muckley, Noll, JF, T-MI, 2015)

For synthesis operator  $\mathbf{x} = \mathbf{Q}\mathbf{z}$  with  $\mathbf{z}$  sparse:

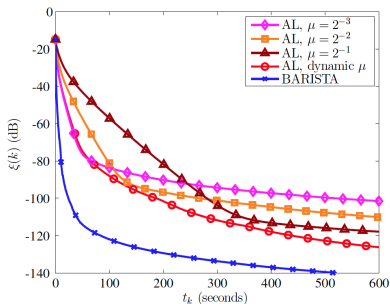
$$\nabla^2 \frac{1}{2} \|\mathbf{y} - \mathbf{F}\mathbf{S}\mathbf{Q}\|_2^2 = \mathbf{Q}'\mathbf{S}'\mathbf{F}'\mathbf{F}\mathbf{S}\mathbf{Q} \leq \mathbf{Q}'\mathbf{S}'\mathbf{S}\mathbf{Q} \leq \mathbf{D}$$

for a suitable diagonal matrix  $\mathbf{D}$ . (cf., SQS)

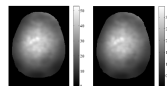
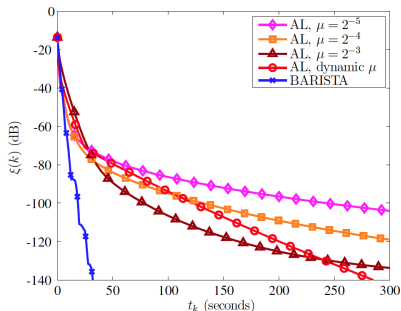
- ▶  $\mathbf{D}^{-1}$  becomes voxel-dependent step size, akin to SQS in CT

“Compressed sensing” MRI reconstruction:

Total variation (TV) regularizer



Undecimated Haar Wavelets



Corresponding  $D$  for each of the two cases:

BARISTA requires no algorithm parameter tuning, unlike AL.

Includes momentum with adaptive restart of O'Donoghue and Candès (2014).

FGM1 is in the general class of first-order methods:

$$\mathbf{x}^{(n+1)} = \mathbf{x}^{(n)} - \frac{1}{L} \sum_{k=0}^n h_{n+1,k} \nabla \Psi(\mathbf{x}^{(k)})$$

where the step-size factors  $\{h_{n,k}\}$  are

$$\begin{bmatrix} 1 & 0 & 0 & 0 & 0 & 0 \\ 0 & 1.25 & 0 & 0 & 0 & 0 \\ 0 & 0.10 & 1.40 & 0 & 0 & 0 \\ 0 & 0.05 & 0.20 & 1.50 & 0 & 0 \\ 0 & 0.03 & 0.11 & 0.29 & 1.57 & 0 \\ \vdots & & & & & \ddots \end{bmatrix}$$

Use of previous gradients  $\implies$  “momentum”

Is this the optimal choice for  $\{h_{n,k}\}$  ?

Can we improve on the constant **2** in worst-case convergence rate?

Drori & Teboulle (2014) numerically found  $2\times$  better  $\{h_{n,k}\}$

# Optimized gradient method (OGM1)

New approach by optimizing  $\{h_{n,k}\}$  analytically

Initialize:  $t_0 = 1, \mathbf{z}^{(0)} = \mathbf{x}^{(0)}$  (Donghwan Kim and JF; 2014, 2015)

$$\mathbf{z}^{(n+1)} = \mathbf{x}^{(n)} - \frac{1}{L} \nabla \Psi(\mathbf{x}^{(n)}) \quad (\text{usual GD update})$$

$$t_{n+1} = \frac{1}{2} \left( 1 + \sqrt{1 + 4t_n^2} \right) \quad (\text{momentum factors})$$

$$\mathbf{x}^{(n+1)} = \mathbf{z}^{(n+1)} + \frac{t_n - 1}{t_{n+1}} \left( \mathbf{z}^{(n+1)} - \mathbf{z}^{(n)} \right) + \underbrace{\frac{t_n}{t_{n+1}} \left( \mathbf{z}^{(n+1)} - \mathbf{x}^{(n)} \right)}_{\text{new momentum}}$$

Smaller (worst-case) convergence bound than Nesterov by  $2\times$ :

$$\Psi(\mathbf{z}^{(n)}) - \Psi(\mathbf{x}^{(*)}) \leq \frac{1L \|\mathbf{x}^{(0)} - \mathbf{x}^{(*)}\|_2^2}{(n+1)^2}.$$

Recently DK found a Huber-like function for which OGM1 achieves that upper bound (thus tight), inspired by numerical work of Taylor *et al.* (2015).

# Example: Image restoration (!?)

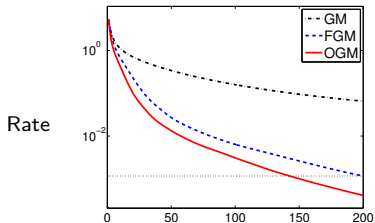
True  
 $x$



Blurry  
 $y$



Restored  
 $\hat{x}$



$\Psi(\mathbf{x}^{(n)}) - \Psi(\hat{\mathbf{x}})$  vs iteration  $n$

## What

CT

MRI

## Why

Why CT iterative

Why MRI iterative

## How

Optimization transfer

Separable quadratic surrogates

Momentum

**Ordered subsets**

## Parallelization

- ▶ Data decomposition (aka incremental gradients, cf. stochastic GD):

$$\Psi(\mathbf{x}) = \sum_{m=1}^M \Psi_m(\mathbf{x}), \quad \Psi_m(\mathbf{x}) \triangleq \underbrace{\frac{1}{2} \|\mathbf{y}_m - \mathbf{A}_m \mathbf{x}\|_{\mathbf{W}_m}^2}_{1/M\text{th of measurements}} + \frac{1}{M} R(\mathbf{x})$$

- ▶ Key idea. For  $\mathbf{x}$  far from minimizer:  $\nabla \Psi(\mathbf{x}) \approx M \nabla \Psi_m(\mathbf{x})$
- ▶ SQS:

$$\mathbf{x}^{(n+1)} = \mathbf{x}^{(n)} - \mathbf{D}^{-1} \nabla \Psi(\mathbf{x}^{(n)})$$

- ▶ OS-SQS:

for  $n = 0, 1, \dots$  (iteration)

for  $m = 1, \dots, M$  (subset)

$k = nM + m$  (subiteration)

$$\mathbf{x}^{k+1} = \mathbf{x}^k - \mathbf{D}^{-1} \underbrace{M \nabla \Psi_m(\mathbf{x}^k)}_{\text{less work}}$$

- ▶ Coil-wise in parallel MRI

(Muckley, Noll, JF, ISMRM 2014)

For more acceleration, combine OGM1 with ordered subsets (OS).

OS-OGM1:

Initialize:  $t_0 = 1$ ,  $\mathbf{z}^{(0)} = \mathbf{x}^{(0)}$

for  $n = 0, 1, \dots$  (iteration)

  for  $m = 1, \dots, M$  (subset)

$k = nM + m$  (subiteration)

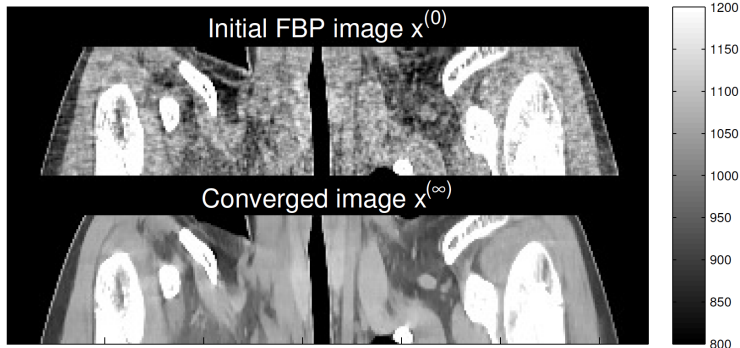
$$\mathbf{z}^{k+1} = \left[ \mathbf{x}^k - \mathbf{D}^{-1} \mathbf{M} \nabla \Psi_m(\mathbf{x}^k) \right]_+ \quad (\text{typical OS-SQS})$$

$$t_{k+1} = \frac{1}{2} \left( 1 + \sqrt{1 + 4t_k^2} \right)$$

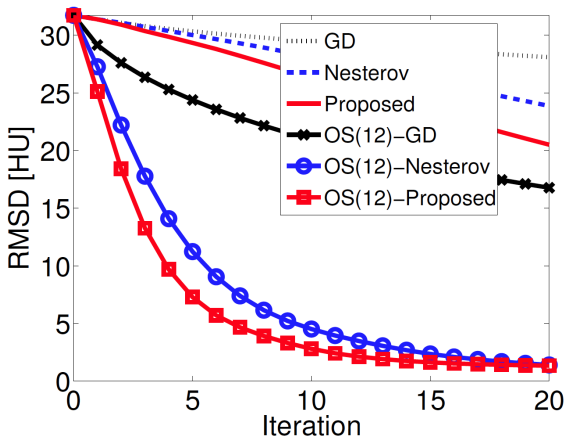
$$\mathbf{x}^{k+1} = \mathbf{z}^{k+1} + \frac{t_k - 1}{t_{k+1}} (\mathbf{z}^{k+1} - \mathbf{z}^k) + \frac{t_k}{t_{k+1}} (\mathbf{z}^{k+1} - \mathbf{x}^k)$$

- ▶ Approximate convergence rate for  $\Psi$ :  $O\left(\frac{1}{n^2 M^2}\right)$   
(Donghwan Kim and JF; CT 2014)
- ▶ Same compute per iteration as other OS methods  
(One forward / backward projection and  $M$  regularizer gradients per iteration)
- ▶ Same memory as OGM1 (two more images than OS-SQS)
- ▶ Guaranteed convergence for  $M = 1$
- ▶ No convergence theory for  $M > 1$ 
  - unstable for large  $M$
  - small  $M$  preferable for parallelization
- ▶ Now fast enough to show X-ray CT examples...

- 3D cone-beam helical X-ray CT scan
- pitch 0.5
- image  $x$ :  $512 \times 512 \times 109$  with 70 cm FOV and 0.625 mm slices
- sinogram :  $y$  888 detectors  $\times$  32 rows  $\times$  7146 views

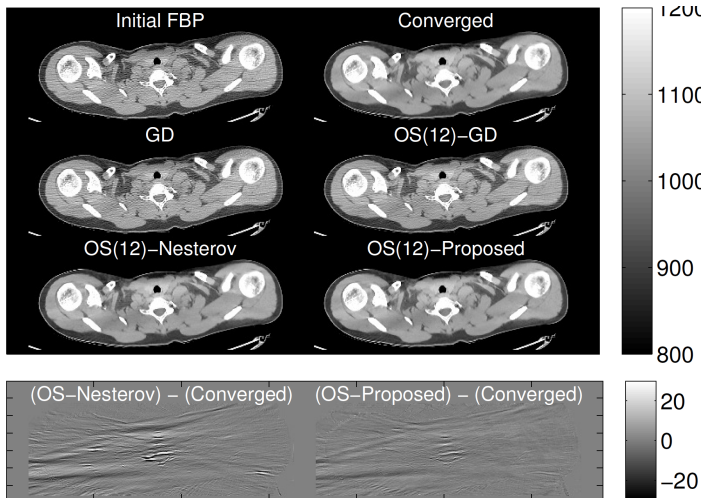


# OS-OGM1 results: convergence rate

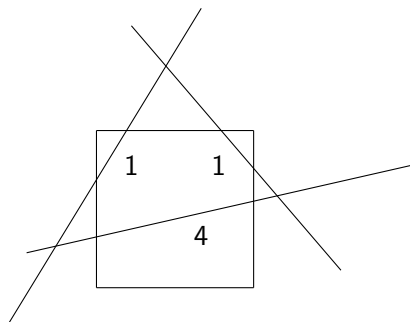


Root mean square difference (RMSD) between  $\mathbf{x}^{(n)}$  and  $\mathbf{x}^{(\infty)}$  over ROI (in HU), versus iteration.

(Compute times per iteration are very similar.)



At iteration  $n = 10$  with  $M = 12$  subsets.



- one-pixel image
- three intersecting rays

- $\mathbf{A} = \begin{bmatrix} 1 \\ 1 \\ 4 \end{bmatrix}$

- $\mathbf{x} = 2, \mathbf{y} = \mathbf{A}\mathbf{x} = \begin{bmatrix} 2 \\ 2 \\ 8 \end{bmatrix}$

- condition number of  $\mathbf{A}'\mathbf{A} = 1$
- consistent system of eqns.

OS-SQS-LS for  $M = 3$  subsets:

$$\mathbf{x}^{\text{new}} = \mathbf{x}^{\text{old}} - \mathbf{D}^{-1} 3 \nabla_m \mathbf{x}^{\text{old}} = \mathbf{x}^{\text{old}} - \mathbf{D}^{-1} 3 \mathbf{A}' (\mathbf{A} \mathbf{x}^{\text{old}} - \mathbf{y})$$

$$\mathbf{D} = \text{diag}\{\mathbf{A}' \mathbf{A} \mathbf{1}\} = 1^2 + 1^2 + 4^2 = 18$$

After 3 updates:

$$\begin{aligned} \mathbf{x}^{(n+1)} - \mathbf{x} &= \left(1 - \frac{3}{18} 1^2\right) \left(1 - \frac{3}{18} 1^2\right) \left(1 - \frac{3}{18} 4^2\right) (\mathbf{x}^{(n)} - \mathbf{x}) \\ &= -2(15/18)^3 (\mathbf{x}^{(n)} - \mathbf{x}) = -\frac{125}{108} (\mathbf{x}^{(n)} - \mathbf{x}) \end{aligned}$$

Divergence of OS-SQS-LS is possible even in well-conditioned, consistent case

## What

CT

MRI

## Why

Why CT iterative

Why MRI iterative

## How

Optimization transfer

Separable quadratic surrogates

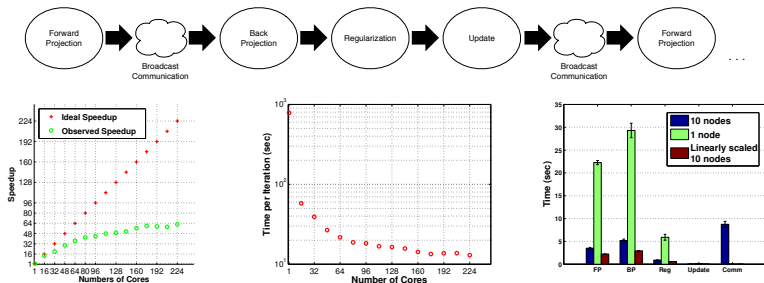
Momentum

Ordered subsets

## Parallelization

Distribute long object (320 useful slices) into (overlapping) slabs (128 slices each) across 5 separate clusters, each with 10 nodes having 16 cores.

Use MPI (message passing interface) for within-cluster communication:



Rosen, Wu, Wenisch, JF (Fully 3D, 2013)

- Overlapping slabs is inefficient
- Communication time (within cluster, after every subset) is serious bottleneck

Conventional OS approach uses a voxel-wise SQS:

$$\begin{aligned} \Psi(\mathbf{x}) &\leq \Psi(\mathbf{x}^{(n)}) + \nabla \Psi(\mathbf{x}^{(n)}) (\mathbf{x} - \mathbf{x}^{(n)}) + \frac{1}{2} (\mathbf{x} - \mathbf{x}^{(n)})' \mathbf{D} (\mathbf{x} - \mathbf{x}^{(n)}) \\ &= \Psi(\mathbf{x}^{(n)}) + \sum_{j=1}^N \frac{\partial}{\partial x_j} \Psi(\mathbf{x}^{(n)}) (x_j - x_j^{(n)}) + \frac{1}{2} d_j (x_j - x_j^{(n)})^2 \end{aligned}$$

Diagonal matrix  $\mathbf{D}$  majorizes the Hessian of  $\Psi$ :  $\nabla^2 \Psi(\mathbf{x}) \preceq \mathbf{D}$ .

Distributed computing alternative: slab-separable surrogate:

$$\Psi(\mathbf{x}) - \Psi(\mathbf{x}^{(n)}) \leq \sum_{b=1}^B \Psi_b(\mathbf{x}_b)$$

$$\Psi_b(\mathbf{x}_b) \triangleq \nabla_{\mathbf{x}_b} \Psi(\mathbf{x}^{(n)}) (\mathbf{x}_b - \mathbf{x}_b^{(n)}) + \frac{1}{2} (\mathbf{x}_b - \mathbf{x}_b^{(n)})' \mathbf{H}_b (\mathbf{x}_b - \mathbf{x}_b^{(n)})$$

Block diagonal matrix  $\mathbf{H} = \text{diag}\{\mathbf{H}_1, \dots, \mathbf{H}_B\}$  majorizes  $\nabla^2 \Psi(\mathbf{x})$ .

$$\Psi_b(\mathbf{x}_b) \triangleq \nabla_{\mathbf{x}_b} \Psi(\mathbf{x}^{(n)}) (\mathbf{x}_b - \mathbf{x}_b^{(n)}) + \frac{1}{2} (\mathbf{x}_b - \mathbf{x}_b^{(n)})' \mathbf{H}_b (\mathbf{x}_b - \mathbf{x}_b^{(n)})$$

$$\mathbf{H}_b \triangleq \mathbf{A}'_b \mathbf{W} \Lambda_b \mathbf{A}_b, \quad \Lambda_b \triangleq \text{diag}\{\mathbf{A}\mathbf{1} \oslash \mathbf{A}_b \mathbf{1}_b\}$$

Updates parallelizable across blocks (slabs):

$$\mathbf{x}_b^{(n+1)} \triangleq \arg \min_{\mathbf{x}_b \succeq \mathbf{0}} \Psi_b(\mathbf{x}_b).$$

- ▶ Reduces communication.
- ▶ (Apply favorite optimization method within slab.)
- ▶ (Donghwan Kim and JF; Fully 3D, 2015) [Mo18]

- 
- 1: Initialize  $\tilde{\mathbf{x}}^{(0)}$  by FBP, and compute  $\mathbf{D}$ .
  - 2: Distribute image  $\tilde{\mathbf{x}}^{(0)}$  and data  $\mathbf{y}$  into  $B$  nodes.
  - 3: **for**  $n = 0, 1, \dots$
  - 4: Minimize  $\phi_{\text{BSS}}(\mathbf{x}; \tilde{\mathbf{x}}^{(n)})$  using  $L$  sub-iterations of OS-SQS-mom.
    - 1) Initialize  $\mathbf{x}^{(0)} = \mathbf{z}^{(0)}$  by  $\tilde{\mathbf{x}}^{(n)}$ , and  $t^{(0)} = 1$ .
    - 2) **for**  $l = 0, 1, \dots, L - 1$
    - 3)  $m = l \bmod M$
    - 4)  $t^{(l+1)} = \frac{1}{2} \left( 1 + \sqrt{1 + 4 [t^{(l)}]^2} \right)$
    - 5) **for**  $b = 1, \dots, B$  **simultaneously**
    - 6)  $\mathbf{g}_{m,b}^{(l)} = M \nabla_b \phi_{\text{BSS},m}(\mathbf{z}_b^{(\frac{l}{M})}; \mathbf{z}^{(0)})$  [subset gradient]
    - 7)  $\mathbf{x}_b^{(\frac{l+1}{M})} = \left[ \mathbf{z}_b^{(\frac{l}{M})} - \mathbf{D}_b^{-1} \mathbf{g}_{m,b}^{(l)} \right]_+$  [OS-SQS update]
    - 8)  $\mathbf{z}_b^{(\frac{l+1}{M})} = \mathbf{x}_b^{(\frac{l+1}{M})} + \frac{t^{(l)} - 1}{t^{(l+1)}} \left( \mathbf{x}_b^{(\frac{l+1}{M})} - \mathbf{x}_b^{(\frac{l}{M})} \right)$  [momentum]
    - 9) **end for**
    - 10) **end for**
    - 11)  $\tilde{\mathbf{x}}^{(n+1)} = \mathbf{x}^{(\frac{l}{M})}$
  - 5: **Communicate**  $\tilde{\mathbf{x}}^{(n+1)}$ .
  - 6: **end for**
-

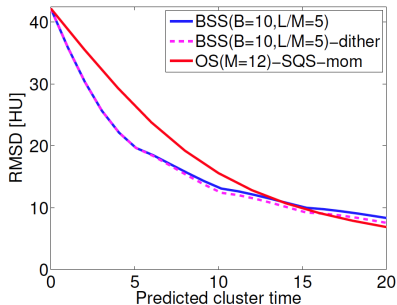
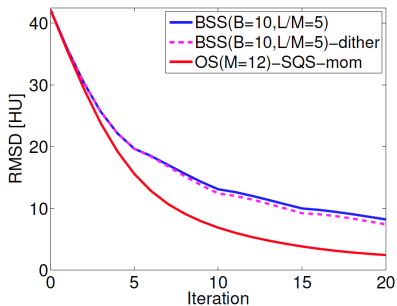
- $256 \times 256 \times 160$  XCAT phantom (Segars *et al.*, 2008)
- Simulated helical CT,  $444 \times 32 \times 492$
- $M = 12$  subsets,  $B = 10$  blocks,  $L = 5$  inner iterations
- Matlab emulation

FBP initializer  $\mathbf{x}^{(0)}$



Converged  $\mathbf{x}^{(\infty)}$

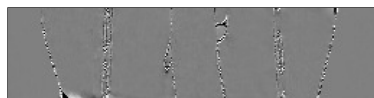




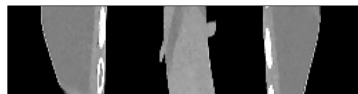
- Outer loop interrupts momentum  
 ⇒ BSS is slower per iteration than OS-OGM
- Reduced communication reduces overall time



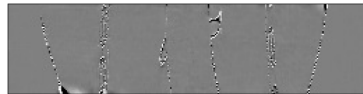
(a)  $\hat{x}^{(10)}$  of OS-SQS-mom( $M=12$ )



(b) Difference between (a) and  $\hat{x}$



(c)  $\hat{x}^{(20)}$  of BSS( $B=10, M=12, L/M=5$ )



(d) Difference between (c) and  $\hat{x}$

- Comparable images
- Algorithm designed for distributed computation

# Duality approach for using GPU

- Data transfer between system RAM and GPU can be bottleneck
- “Hide” communication time by overlapping with computation

Algorithm synopsis: (Madison McGaffin and JF; Fully 3D, 2015) [Wed. AM]

- Write cost function  $\Psi(\mathbf{x})$  in terms of dual variables  $\mathbf{v}$  and  $\mathbf{u}$  for data-fit and regularizer:

$$\Psi(\mathbf{x}) = \sum_{i=1}^M h_i([\mathbf{A}\mathbf{x}]_i) + \sum_k \psi([\mathbf{C}\mathbf{x}]_k)$$

$$\mathbf{x}^{(n+1)} = \arg \min_{\mathbf{x}} \sup_{\mathbf{u}, \mathbf{v}}$$

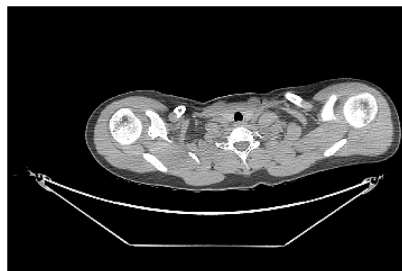
$$(\mathbf{A}'\mathbf{u} + \mathbf{C}'\mathbf{v})' \mathbf{x} - \sum_{i=1}^M h_i^*(u_i) - \sum_k \psi^*(v_k) + \frac{\mu}{2} \|\mathbf{x} - \mathbf{x}^{(n)}\|_2^2$$

$h_i^*$  and  $\psi^*$  denote convex conjugates of  $h_i$  and  $\psi$

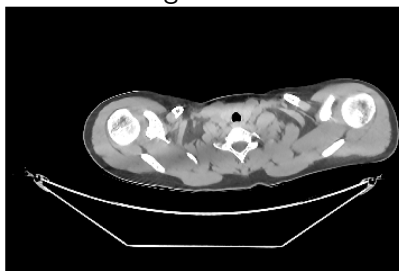
- Alternate between updating
  - several projection view dual variables  $\{u_i\}$
  - dual variables for one regularization direction  $\{v_k\}$
- Using dual variables “decouples” regularizer and data terms

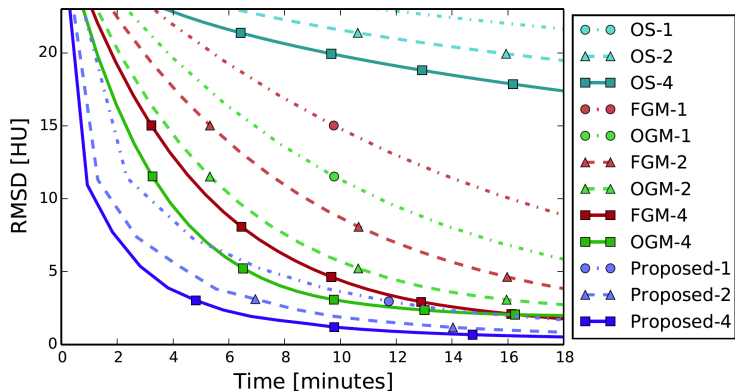
- 3D cone-beam helical X-ray CT scan
- pitch 0.5
- image  $\mathbf{x}$ :  $512 \times 512 \times 109$  with 70 cm FOV and 0.625 mm slices
- sinogram :  $\mathbf{y}$  888 detectors  $\times$  32 rows  $\times$  7146 views
- OpenCL on aging NVIDIA GTX 480 GPU with 2.5 GB RAM

FBP initializer  $\mathbf{x}^{(0)}$

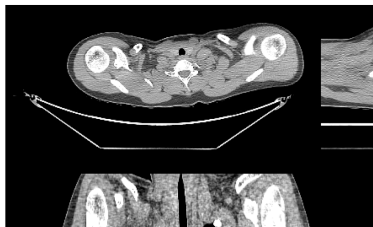


Converged  $\mathbf{x}^{(\infty)}$

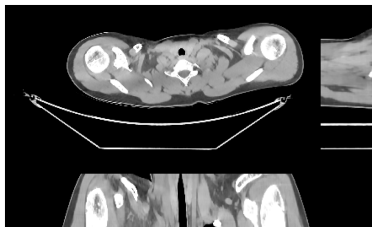




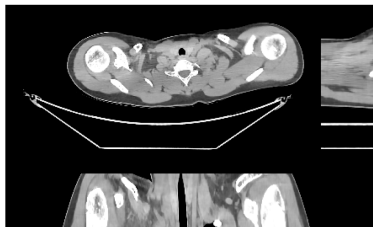
- Algorithm designed specifically for GPU architecture characteristics
- Future work:
  - combine with BSS for multiple nodes ?



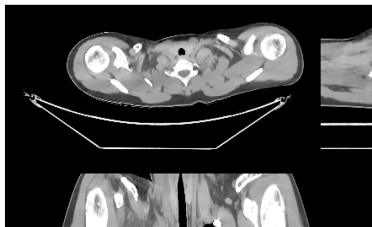
(a) Filtered backprojection



(b) Reference



(c) OS-OGM with 4 GPUs after 8 iterations (5.2 minutes)



(d) Proposed with 4 GPUs after 5 iterations (4.8 minutes)

- ▶ Model-based image reconstruction can
  - improve image quality for low-dose X-ray CT
  - enable faster MRI scans via under-sampling
- ▶ Much more: dynamic image reconstruction, motion compensation, ...
- ▶ Computation time remains a significant challenge
- ▶ Moore's law will not solve the problem
- ▶ Algorithms designed for distributed computation are essential
  - Block-separable surrogates to reduce communication  
(Donghwan Kim and JF; Fully 3D, 2015) [Mo18]
  - Duality approach to overlap communication with computation  
Also provides a OS-like algorithm with convergence theory  
(Madison McGaffin and JF; Fully 3D, 2015) [Wed. AM]

- \* G. Hounsfield, *A method of apparatus for examination of a body by radiation such as x-ray or gamma radiation*, US Patent 1283915. British patent 1283915, London., 1972.
- \* R. Gordon, R. Bender, and G. T. Herman, "Algebraic reconstruction techniques (ART) for the three-dimensional electron microscopy and X-ray photography," *J. Theor. Biol.*, vol. 29, no. 3, 471–81, Dec. 1970.
- \* R. Gordon and G. T. Herman, "Reconstruction of pictures from their projections," *Comm. ACM*, vol. 14, no. 12, 759–68, Dec. 1971.
- \* G. T. Herman, A. Lent, and S. W. Rowland, "ART: mathematics and applications (a report on the mathematical foundations and on the applicability to real data of the algebraic reconstruction techniques)," *J. Theor. Biol.*, vol. 42, no. 1, 1–32, Nov. 1973.
- \* R. Gordon, "A tutorial on ART (algebraic reconstruction techniques)," *IEEE Trans. Nuc. Sci.*, vol. 21, no. 3, 78–93, Jun. 1974.
- \* R. L. Kashyap and M. C. Mittal, "Picture reconstruction from projections," *IEEE Trans. Comp.*, vol. 24, no. 9, 915–23, Sep. 1975.
- \* A. J. Rockmore and A. Macovski, "A maximum likelihood approach to transmission image reconstruction from projections," *IEEE Trans. Nuc. Sci.*, vol. 24, no. 3, 1929–35, Jun. 1977.
- \* K. Lange and R. Carson, "EM reconstruction algorithms for emission and transmission tomography," *J. Comp. Assisted Tomo.*, vol. 8, no. 2, 306–16, Apr. 1984.
- \* K. Sauer and C. Bouman, "A local update strategy for iterative reconstruction from projections," *IEEE Trans. Sig. Proc.*, vol. 41, no. 2, 534–48, Feb. 1993.
- \* S. H. Manglos, G. M. Gagne, A. Krol, F. D. Thomas, and R. Narayanaswamy, "Transmission maximum-likelihood reconstruction with ordered subsets for cone beam CT," *Phys. Med. Biol.*, vol. 40, no. 7, 1225–41, Jul. 1995.

- \* C. Kamphuis and F. J. Beekman, "Accelerated iterative transmission CT reconstruction using an ordered subsets convex algorithm," *IEEE Trans. Med. Imag.*, vol. 17, no. 6, 1001–5, Dec. 1998.
- \* H. Erdoğan and J. A. Fessler, "Ordered subsets algorithms for transmission tomography," *Phys. Med. Biol.*, vol. 44, no. 11, 2835–51, Nov. 1999.
- \* E. Hansis, J. Bredno, D. Sowards-Emmerd, and L. Shao, "Iterative reconstruction for circular cone-beam CT with an offset flat-panel detector," in *Proc. IEEE Nuc. Sci. Symp. Med. Im. Conf.*, 2010, 2228–31.
- \* B. P. Sutton, D. C. Noll, and J. A. Fessler, "Fast, iterative image reconstruction for MRI in the presence of field inhomogeneities," *IEEE Trans. Med. Imag.*, vol. 22, no. 2, 178–88, Feb. 2003.
- \* ———, "Dynamic field map estimation using a spiral-in / spiral-out acquisition," *Mag. Res. Med.*, vol. 51, no. 6, 1194–204, Jun. 2004.
- \* V. T. Olafsson, D. C. Noll, and J. A. Fessler, "Fast joint reconstruction of dynamic  $R_2^*$  and field maps in functional MRI," *IEEE Trans. Med. Imag.*, vol. 27, no. 9, 1177–88, Sep. 2008.
- \* Y. Censor, D. E. Gustafson, A. Lent, and H. Tuy, "A new approach to the emission computerized tomography problem: simultaneous calculation of attenuation and activity coefficients," *IEEE Trans. Nuc. Sci.*, vol. 26, no. 2, 2775–9, Apr. 1979.
- \* N. H. Clinthorne, J. A. Fessler, G. D. Hutchins, and W. L. Rogers, "Joint maximum likelihood estimation of emission and attenuation densities in PET," in *Proc. IEEE Nuc. Sci. Symp. Med. Im. Conf.*, vol. 3, 1991, 1927–32.
- \* H. Erdoğan and J. A. Fessler, "Algorithms for joint estimation of attenuation and emission images in PET," in *Proc. IEEE Conf. Acoust. Speech Sig. Proc.*, vol. 6, 2000, 3783–6.
- \* A. Rezaei, M. Defrise, and J. Nuyts, "ML-reconstruction for TOF-PET with simultaneous estimation of the attenuation factors," *IEEE Trans. Med. Imag.*, vol. 33, no. 7, 1563–72, Jul. 2014.
- \* C. Yip, J. A. Fessler, and D. C. Noll, "Iterative RF pulse design for multidimensional, small-tip-angle selective excitation," *Mag. Res. Med.*, vol. 54, no. 4, 908–17, Oct. 2005.

- \* F. Zhao, J. A. Fessler, S. M. Wright, and D. C. Noll, "Regularized estimation of magnitude and phase of multi-coil B1 field via Bloch-Siegert B1 mapping and coil combination optimizations," *IEEE Trans. Med. Imag.*, vol. 33, no. 10, 2020–30, Oct. 2014.
- \* S. S. Vasanawala, M. T. Alley, B. A. Hargreaves, R. A. Barth, J. M. Pauly, and M. Lustig, "Improved pediatric MR imaging with compressed sensing," *Radiology*, vol. 256, 607–16, 2010.
- \* K. P. Pruessmann, M. Weiger, M. B. Scheidegger, and P. Boesiger, "SENSE: sensitivity encoding for fast MRI," *Mag. Res. Med.*, vol. 42, no. 5, 952–62, Nov. 1999.
- \* M. Lustig, D. L. Donoho, J. M. Santos, and J. M. Pauly, "Compressed sensing MRI," *IEEE Sig. Proc. Mag.*, vol. 25, no. 2, 72–82, Mar. 2008.
- \* S. Ramani and J. A. Fessler, "Parallel MR image reconstruction using augmented Lagrangian methods," *IEEE Trans. Med. Imag.*, vol. 30, no. 3, 694–706, Mar. 2011.
- \* A. R. De Piero, "A modified expectation maximization algorithm for penalized likelihood estimation in emission tomography," *IEEE Trans. Med. Imag.*, vol. 14, no. 1, 132–7, Mar. 1995.
- \* Y. Drori and M. Teboulle, "Performance of first-order methods for smooth convex minimization: A novel approach," *Mathematical Programming*, vol. 145, no. 1-2, 451–82, Jun. 2014.
- \* Y. Nesterov, "A method for unconstrained convex minimization problem with the rate of convergence  $O(1/k^2)$ ," *Dokl. Akad. Nauk. USSR*, vol. 269, no. 3, 543–7, 1983.
- \* ———, "Smooth minimization of non-smooth functions," *Mathematical Programming*, vol. 103, no. 1, 127–52, May 2005.
- \* D. Kim and J. A. Fessler, *Optimized first-order methods for smooth convex minimization*, arxiv 1406.5468, 2014.
- \* ———, "Optimized first-order methods for smooth convex minimization," *Mathematical Programming*, 2015, Submitted.

- \* M. J. Muckley, D. C. Noll, and J. A. Fessler, "Fast parallel MR image reconstruction via B1-based, adaptive restart, iterative soft thresholding algorithms (BARISTA)," *IEEE Trans. Med. Imag.*, vol. 34, no. 2, 578–88, Feb. 2015.
- \* B. O'Donoghue and E. Candès, "Adaptive restart for accelerated gradient schemes," *Found. Computational Math.*, 2014.
- \* D. Kim and J. A. Fessler, "An optimized first-order method for image restoration," in *Proc. IEEE Intl. Conf. on Image Processing*, To appear., 2015.
- \* A. B. Taylor, J. M. Hendrickx, and François. Glineur, *Smooth strongly convex interpolation and exact worst-case performance of first-order methods*, arxiv 1502.05666, 2015.
- \* M. Muckley, D. C. Noll, and J. A. Fessler, "Accelerating SENSE-type MR image reconstruction algorithms with incremental gradients," in *Proc. Intl. Soc. Mag. Res. Med.*, 2014, p. 4400.
- \* D. Kim and J. A. Fessler, "Optimized momentum steps for accelerating X-ray CT ordered subsets image reconstruction," in *Proc. 3rd Intl. Mtg. on image formation in X-ray CT*, 2014, 103–6.
- \* J. M. Rosen, J. Wu, T. F. Wenisch, and J. A. Fessler, "Iterative helical CT reconstruction in the cloud for ten dollars in five minutes," in *Proc. Intl. Mtg. on Fully 3D Image Recon. in Rad. and Nuc. Med.*, 2013, 241–4.
- \* D. Kim and J. A. Fessler, "Distributed block-separable ordered subsets for helical X-ray CT image reconstruction," in *Proc. Intl. Mtg. on Fully 3D Image Recon. in Rad. and Nuc. Med.*, To appear., 2015.
- \* W. P. Segars, M. Mahesh, T. J. Beck, E. C. Frey, and B. M. W. Tsui, "Realistic CT simulation using the 4D XCAT phantom," *Med. Phys.*, vol. 35, no. 8, 3800–8, Aug. 2008.
- \* M. G. McGaffin and J. A. Fessler, "Fast GPU-driven model-based X-ray CT image reconstruction via alternating dual updates," in *Proc. Intl. Mtg. on Fully 3D Image Recon. in Rad. and Nuc. Med.*, To appear., 2015.